



# Quantifying the link between crack distribution and resistance spot weld strength reduction in liquid metal embrittlement susceptible steels

E. Wintjes<sup>1</sup> · C. DiGiovanni<sup>1</sup> · L. He<sup>1</sup> · E. Biro<sup>1</sup> · N. Y. Zhou<sup>1</sup>

Received: 21 November 2018 / Accepted: 2 February 2019 / Published online: 13 February 2019  
© International Institute of Welding 2019

## Abstract

Zinc-coated advanced high-strength steels (AHSS) used in the automotive industry are vulnerable to liquid metal embrittlement (LME) during welding. In this work, a “crack index” is used to link LME crack distributions in resistance spot welds to the weld performance. Other commonly used LME metrics, such as maximum crack length, are unable to predict an effect on weld performance. Because both crack size and location have been established as critical characteristics for loss in weld strength, both of these factors must be taken into account when characterizing LME severity. The crack lengths measured in LME-affected welds were observed to fit a lognormal distribution; therefore, the lognormal median is used as the parameter to account for crack size. Long cracks are more likely to adversely impact mechanical performance. Number of cracks can be used to account for the probability that a crack will be found in a critical location. These parameters are multiplied together and divided by the sheet thickness to produce the crack index. A large crack indicates that LME cracks in the weld are likely to impact the mechanical performance of the weld. A simpler version of the crack index may be calculated using the normal median.

**Keywords** Liquid metal embrittlement · Advanced high-strength steel · Resistance spot welding · Weld strength · Cracking

## 1 Introduction

Growing concerns over the impact of fossil fuels on climate change have led to demand for the production of fuel efficient vehicles [1–4]. Consequently, this has led to the development of advanced high-strength steels (AHSS). Parts manufactured from AHSS can be made using thinner sheets due to their superior strength, which can reduce vehicle weight, improving fuel efficiency [5, 6]. These steels are typically coated with zinc to protect against corrosion.

AHSS are commonly joined using resistance spot welding (RSW) during automotive manufacturing. In this process, an electrical current is passed through the sheets of metal and resistive (Joule) heating causes melting at the interface

between the sheets, which solidifies into a weld nugget [7]. During welding, the zinc coating melts at a temperature (419 °C) far below the melting point of steel (~1500 °C). Because of this, liquid zinc may penetrate into the grain boundaries in the heat-affected zone in a process known as liquid metal embrittlement (LME) [8–11]. LME weakens the grain boundaries, causing nucleation of surface cracks, which can propagate as stresses from welding cause the cracks to open up [8, 12, 13].

The impact of LME cracking on weld mechanical performance is currently unclear. A number of studies have indicated that heat-affected zone cracking, including LME cracking, does not have a significant effect on tensile or fatigue properties of resistance spot welds [9, 14–18]. However, several recent studies have also reported that LME cracks do reduce weld mechanical performance of RSW joined high-strength AHSS during tensile lap shear testing, when compared to welds of uncoated material [19–21]. Choi et al. observed that spot welds with LME cracks greater than 325 μm in length demonstrated reduced mechanical performance [19], while DiGiovanni et al. established that crack location plays a role in whether an LME crack will impact tensile lap shear strength in a particular weld [20, 21]. However, no further attempt has been made at determining a quantitative relationship between

---

Recommended for publication by Commission III - Resistance Welding, Solid State Welding, and Allied Joining Process

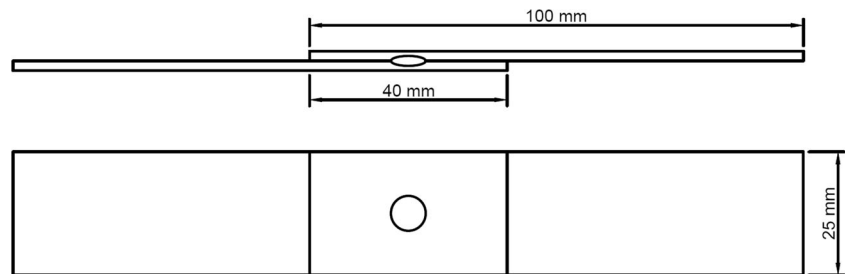
---

✉ E. Wintjes  
elwintje@uwaterloo.ca

<sup>1</sup> Department of Mechanical and Mechatronics Engineering,  
University of Waterloo, 200 University Ave. W., Waterloo, ON N2L  
3G1, Canada

**Table 1** Composition and sheet thickness of AHSS

Material	Thickness (mm)	C (wt%)	Mn (wt%)	Si (wt%)	Al (wt%)	Cr (wt%)	Mo (wt%)	Fe (wt%)
DP980	1.2	0.10	2.1	0.3	0.05	0.2	0.3	Bal.
TRIP690	1.2	0.20	1.7	0.4	1.31	–	–	Bal.
TRIP1100	1.6	0.20	2.2	1.6	–	–	–	Bal.
TRIP1200	1.6	0.22	2.3	1.7	–	0.1	–	Bal.

**Fig. 1** Tensile lap shear coupon geometry

weld strength and LME cracking severity. This task is complicated by the fact that no standard method exists to quantify LME cracking severity in RSW. Methods which have previously been used include maximum crack length [8, 11, 19, 20, 22, 23], total length of surface cracks [10], total crack surface area [24], surface cracking ratio [9], number of LME cracks per weld [23], and mean crack length [12]. None of these metrics have been linked to weld performance; they only describe crack size or distribution. The goal of this study is to establish a metric for LME cracking severity which explains

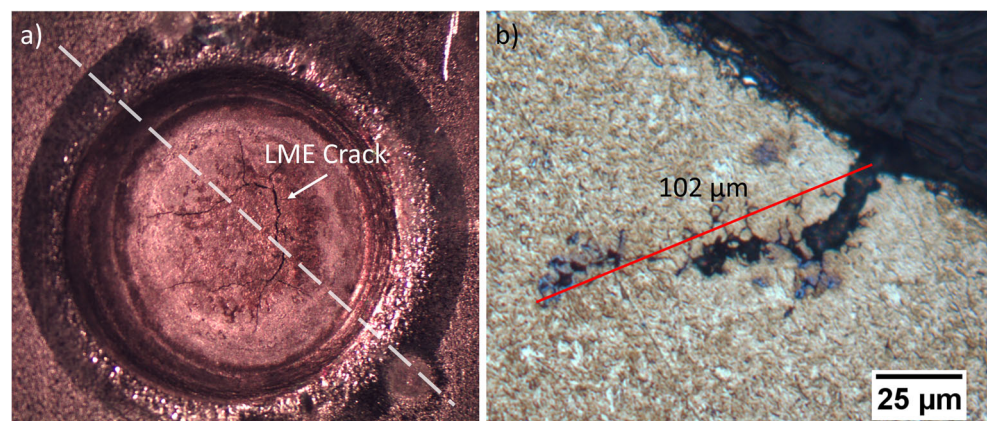
the effect of LME on lap shear strength in RSW of similar materials.

## 2 Materials and methods

Four different grades of hot-dip galvanized AHSS, chosen due to industrial interest, were used for this study: DP980, TRIP690, TRIP1100, and TRIP1200. Their chemical compositions and sheet thicknesses can be found in Table 1. The

**Table 2** Welding parameters used to determine LME susceptibility of AHSS

Material	Electrode diameter (mm)	Force (kN)	Cooling (L/min)	Weld time (cy)	Expulsion current (kA)
DP980	6	4	4	16	10
TRIP690	6	3.6	4	16	10
TRIP1100	7	5.5	6	12-2-12	10
TRIP1200	7	5.5	6	12-2-12	10.5

**Fig. 2** **a** Selection of cross-section plane using visible surface cracks. **b** Measurement of LME crack lengths



**Table 3** Comparison of nugget diameters of welds made with coated vs uncoated AHSS

Material	Nugget diameter (mm)	
	Uncoated	Coated
DP980	6.7	6.6
TRIP690	6.8	6.5
TRIP1100	7.6	7.8
TRIP1200	7.6	7.4

sheets were cut into coupons 25 mm × 25 mm for crack analysis and 25 mm × 100 mm for tensile lap shear testing. The rolling direction is along the 100 mm length of the coupon. A schematic of the lap shear tensile coupons is shown in Fig. 1. All coupons were cleaned with ethanol prior to welding.

Samples were welded using a medium frequency direct current pedestal welder with class 2, female B-type electrode

caps. The expulsion current, defined as the lowest current at which expulsion was observed for three consecutive welds, was determined for each material and is denoted as  $I_{\max}$ . For preliminary testing, each material was welded using a current 10% higher than the expulsion current (denoted as  $I_{\max} + 10\%$ ) to encourage LME cracking. All other welding parameters were selected according to AWS D8.9 [25] and are shown in Table 2. Following preliminary testing, additional samples were welded with currents between  $I_{\max}$  and  $I_{\max} + 10\%$  in increments of 0.2 kA for TRIP 1100 and TRIP1200 to vary the amount of LME cracking. Welding currents above the expulsion current were used because it has been observed that LME becomes more severe with expulsion [26]. DP980 and TRIP690 samples were also welded with an alternating current pedestal welder, as AC welds display different patterns of cracking.

For each condition, five samples were welded for crack analysis. These were cross-sectioned through the most severe

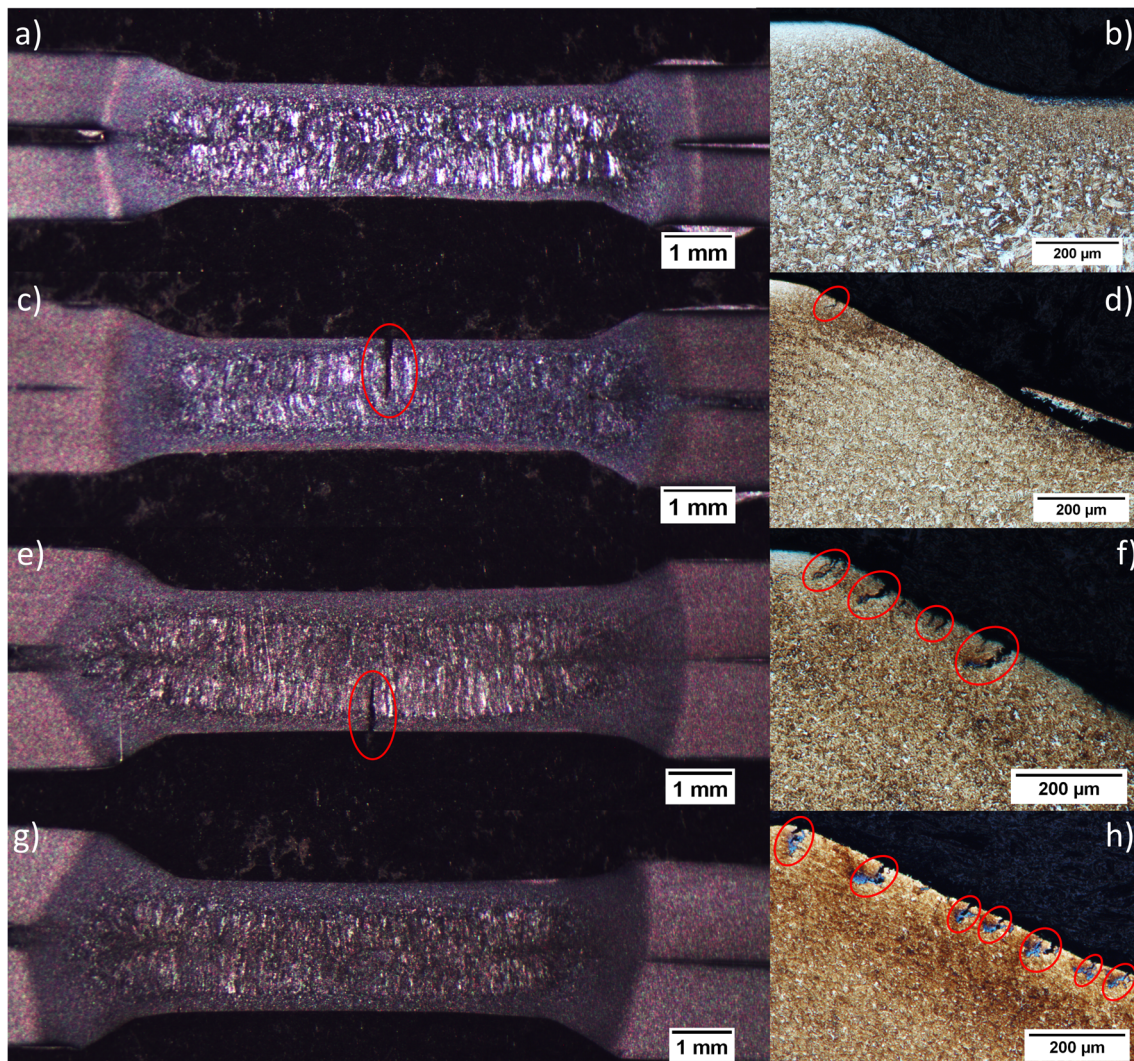
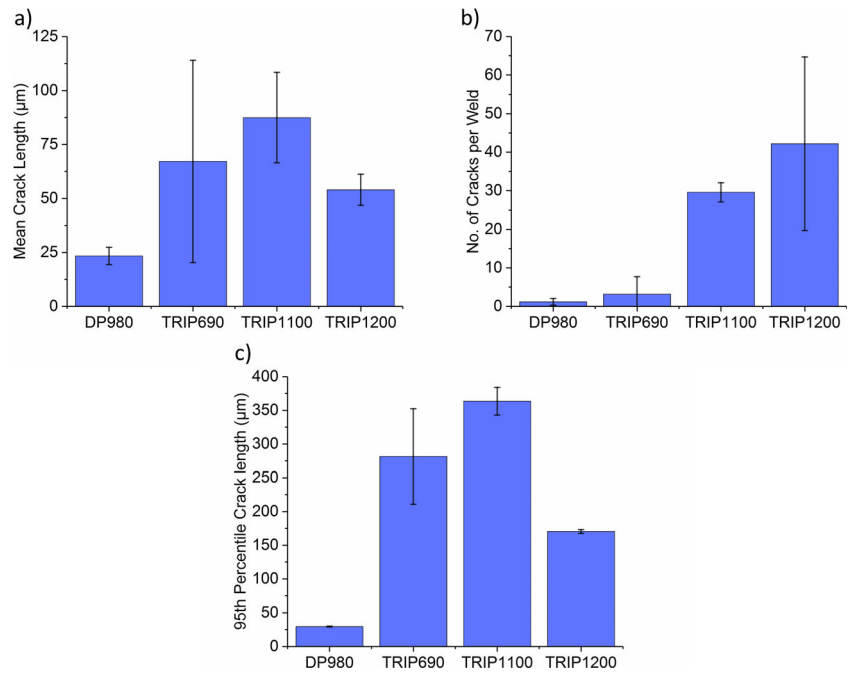


**Fig. 3** Micrographs of resistance spot welds of DP980 (a, b), TRIP690 (c, d), TRIP1100 (e, f), and TRIP1200 (g, h) welded at  $I_{\max} + 10\%$  with LME cracks circled

**Fig. 4** **a** Mean crack length, **b** Average number of cracks per weld, and **c** 95th percentile crack length in samples of AHSS welded at  $I_{max} + 10\%$



cracks visible on the weld surface (Fig. 2a). The cross sections were mounted, polished to a 1-µm diamond finish, and etched with a 5% nital solution. Optical microscope images were taken of any LME cracks in the cross-sections, which were measured using the open source software ImageJ, created by the National Institutes of Health. Cracks were measured with a straight line from the crack opening to the crack tip, as shown in Fig. 2b. The metrics used to quantify LME cracking severity were average number of cracks per weld, arithmetic mean (mean) crack length, and 95th percentile crack length. 95th percentile crack length was selected rather than maximum crack length, which has been used in literature, to prevent the inclusion of outliers.

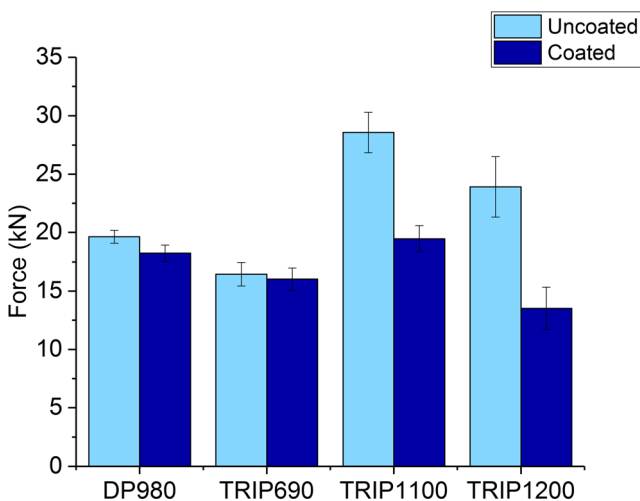


**Fig. 5** Comparison of peak load for coated vs uncoated AHSS welded at  $I_{max} + 10\%$

For each condition, 10 samples were welded for tensile testing: five samples with zinc coating and five which had their coating stripped by pickling in a solution of 20% HCl. The coated and uncoated materials were confirmed to have similar nugget diameters to allow a strength comparison between the two coating conditions (Table 3). The samples were tensile-tested at a rate of 2 mm/min. The percent difference in maximum load between the coated and uncoated samples compared to the weld strength of the uncoated material was calculated to determine the impact of LME cracking on mechanical performance.

To calculate the uncertainty associated with the percent difference in strength, the uncertainty associated with the strengths of the coated and uncoated materials was calculated and standard error propagation techniques were applied as follows:

$$\sigma_{\%Diff} = |\%Diff| \sqrt{\left(\frac{\sigma_{coated}}{F_{coated}}\right)^2 + \left(\frac{\sigma_{uncoated}}{F_{uncoated}}\right)^2} \tag{1}$$

where  $F$  represents the peak load measured by the tensile test and  $\sigma$  represents the standard deviation of the peak load [27]. Ninety-five percent confidence intervals for all mean values were calculated using the equation

$$X \pm 1.96 \frac{\sigma}{\sqrt{N}} \tag{2}$$

where  $X$  is the mean value of the measured quantity,  $\sigma$  is the standard deviation, and  $N$  is the number of measurements. Confidence intervals on 95th percentile and median values were estimated using the bootstrap method [28]. The confidence intervals are displayed as error bars on the graphs.

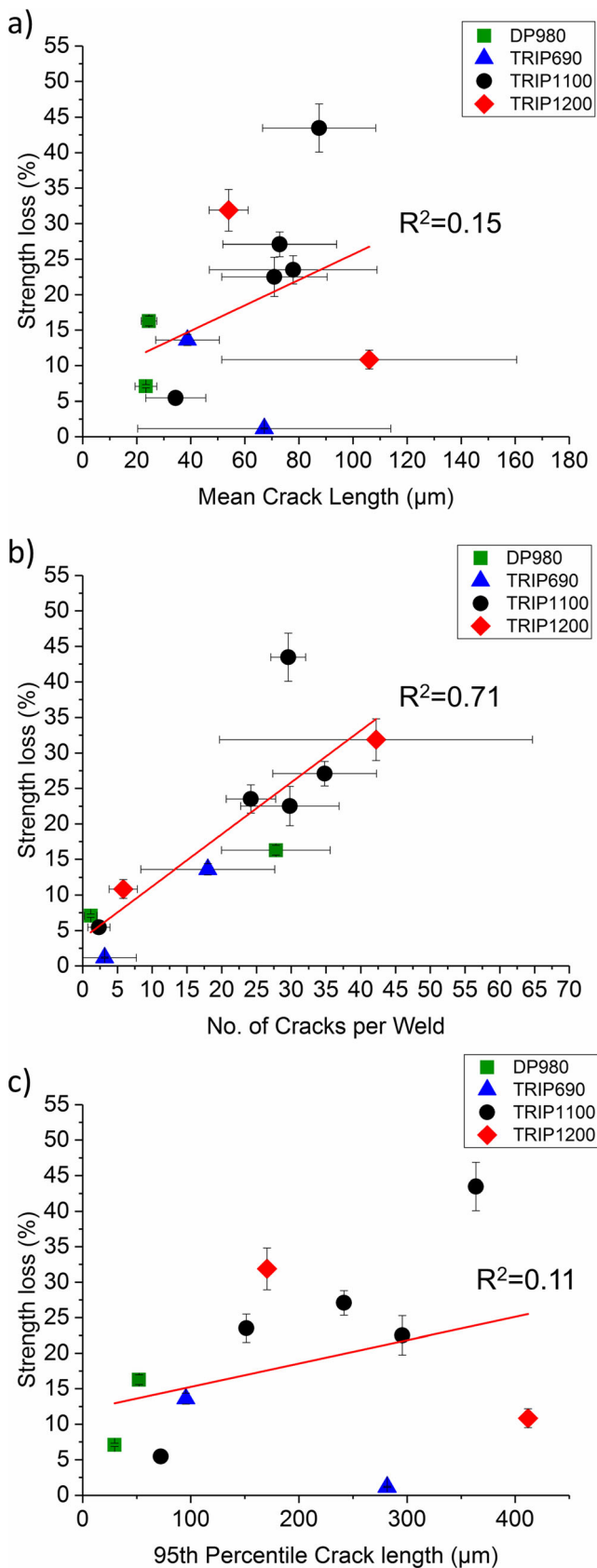


**Fig. 6** Relationship between **a** mean crack length, **b** number of cracks per weld, and **c** 95th percentile crack length and weld strength loss for resistance spot welded AHSS

## 3 Results and discussion

### 3.1 Crack analysis

Each of the four materials tested displayed a different pattern of crack susceptibility. Very few cracks were seen in DP980, and those that were observed were small (Fig. 3a, b). In TRIP690, a few very large cracks were observed (Fig. 3c) but not many cracks were seen in general. In TRIP1100, some very large cracks were observed (Fig. 3e) and many small cracks were also observed in the weld shoulder (Fig. 3f). For TRIP1200, a large number of cracks were observed, which were mostly small and located in the weld shoulder (Fig. 3h).

LME cracking severity has been characterized by the mean crack length, number of cracks per weld, and 95th percentile crack length. Due to their large standard deviations, these quantities fail to capture differences in LME cracking between different conditions. This is evident when comparing the mean crack lengths for the four materials used in this study welded at  $I_{max} + 10\%$ . In particular, the mean crack length in TRIP690 has such large error bars that there is no clear difference between it and any of the other materials (Fig. 4a). In addition, if observing only mean crack length or 95th percentile crack length, it would be concluded that TRIP1100 is the most susceptible to LME of the four materials, while number of cracks would lead to the conclusion that TRIP1200 is the most susceptible (Fig. 4). This is consistent with what was observed in the micrographs in Fig. 3; TRIP1100 and TRIP690 displayed some very large cracks, while TRIP1200 showed a large number of small cracks. The three cracking metrics do not show the same trend of cracking susceptibility, which suggests that a single one of these metrics is not enough to give a complete picture of LME cracking severity.

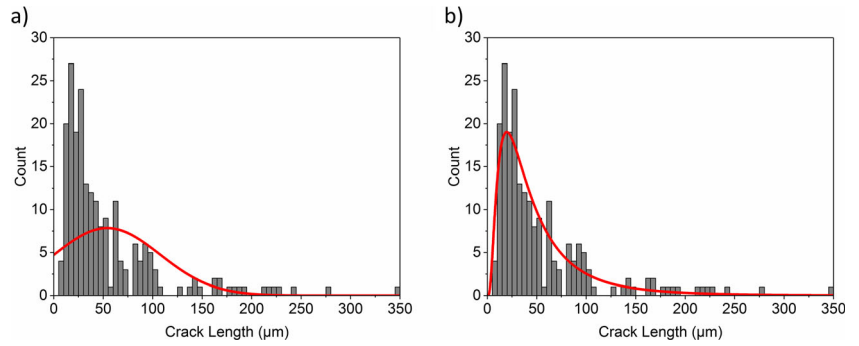
### 3.2 Tensile lap shear testing

Peak loads obtained from tensile-testing the preliminary welds made using a current of  $I_{max} + 10\%$  were compared for welds in materials that were zinc-coated (LME susceptible) and uncoated (LME free). The joint strength was reduced for the coated welds in TRIP1100 and TRIP1200, while LME had almost no effect on the strengths of joints in DP980 and TRIP690 (Fig. 5).

None of the standard crack characterization metrics (mean crack length, number of cracks per weld, 95% percentile crack length) can explain the trend in decreasing strength. In general, longer cracks and a larger number of cracks correspond to a larger decrease in weld strength (Fig. 6); however, there is a large amount of noise when trend lines are fit to the data. In addition, crack location has been shown to have an impact on the weld strength reduction. In a study by DiGiovanni et al., it was shown that cracks around the periphery of the weld propagate and contribute to the weld fracture path, while those in



**Fig. 7** Histogram of LME cracks observed in TRIP1200 fitted with a normal distribution (a) and a lognormal distribution (b)



the center remain unaffected by tensile lap shear testing [20]. The direction of load also determines whether a crack will have an adverse effect on weld strength [21]. This location effect cannot be accounted for using a simple metric like mean crack length or cracks per weld. Even though neither length nor number can fully predict the loss in strength, both clearly have an effect on the weld performance.

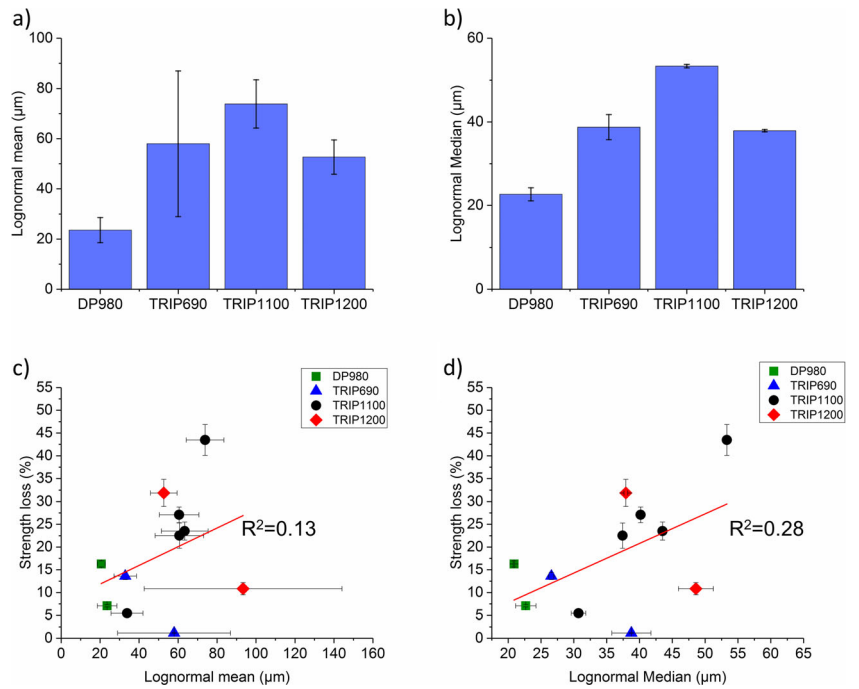
### 3.3 Crack population distributions

Mean crack length is a commonly used descriptor of “typical” crack size in a population. However, as shown in Fig. 4a, this may not be an accurate metric for describing crack size, due to the very large error bars. This is because the use of the mean crack length to describe cracking assumes that the crack populations are normally distributed. When observing the total population of cracks in a weld, it becomes clear that normality is not a good assumption for LME crack populations. The histogram in Fig. 7a shows the actual crack population observed in samples of TRIP1200 welded at  $I_{max} + 10\%$ , while

the curve shows an ideal normal distribution for a population with the same mean, standard deviation, and number of measurements. It is apparent that the normal distribution does not fit the data. However, when compared with the lognormal distribution, the fit is much more accurate (Fig. 7b). This indicates that lognormal statistics should be used to describe LME crack populations.

Using the lognormal mean shows a slight improvement over the arithmetic mean in describing the cracking populations, as the error bars are smaller than those for the arithmetic mean in Fig. 4a. However, a much more significant improvement is seen when the lognormal median is used instead (Fig. 8). This confirms that the lognormal distribution is better able to describe the data than the normal distribution and allows conclusions to be made with greater confidence. Plotting the lognormal median against the weld strength decrease shows a clearer increasing trend than the lognormal mean (Fig. 8c) or normal mean and 95th percentile crack length shown in Fig. 4. However, the lognormal median alone is still not a good predictor of weld strength loss (Fig. 8d).

**Fig. 8** a Lognormal mean and b lognormal median of samples welded at  $I_{max} + 10\%$ . Relationship between c lognormal mean and strength loss and d lognormal median and strength loss in resistance spot welded AHSS



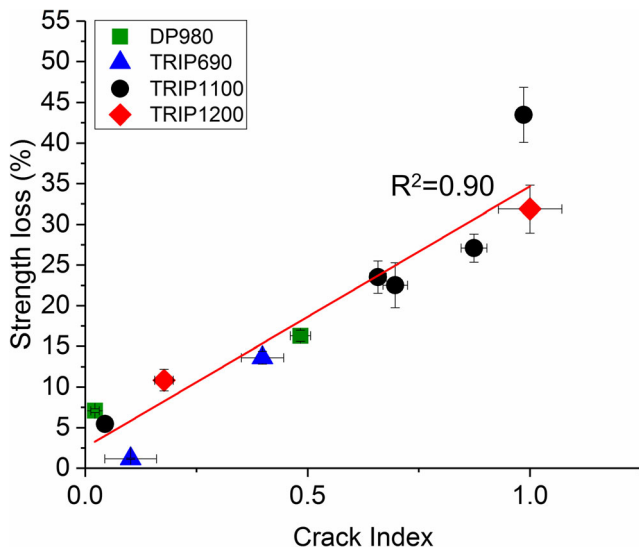


Fig. 9 Relationship between crack index and strength loss for AHSS

### 3.4 Crack index

It is clear that both crack length and number of cracks have an impact on weld strength, although neither can fully describe weld strength loss on their own. Currently, no method exists to predict the location of LME cracks in a weld; however, as the number of cracks increases, the probability that a crack will be located in a critical position also increases. Therefore, multiplying lognormal median crack length by the number of cracks per weld is a way to account for the probability that a crack will be found in a critical location, while the lognormal median determines whether this crack is likely to be of sufficient length to cause a loss in strength. It is necessary to take a probabilistic approach because both crack analysis and tensile lap shear testing are destructive tests. That is, the weld which is analyzed for cracks is not the same weld that is tensile-tested. In addition, the critical crack length for strength loss will depend on the sheet thickness of the metal. Therefore, a “crack index” can be calculated:

$$\text{Crack index} = \frac{nL}{t} \tag{3}$$

where  $n$  is the number of cracks per weld,  $L$  is the lognormal median crack length, and  $t$  is the sheet thickness. This may be thought of physically as a ratio of the total length of cracks in the cross section to the sheet thickness.

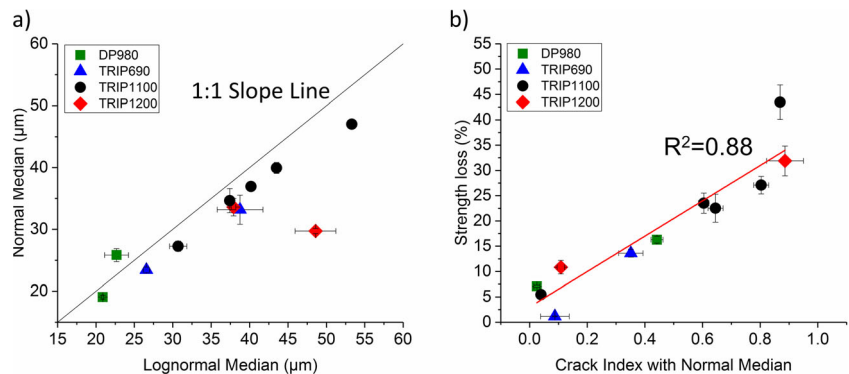
The crack index can be used to accurately assess LME crack severity in resistance spot welds. Graphing the strength decrease against the crack index reveals a linear relationship (Fig. 9). This crack index can be used to predict weld strength loss because it takes into account both crack length and location.

The crack index performs well in explaining the strength loss caused by LME cracks. However, the use of lognormal statistical analysis may be complicated for those who are unfamiliar with this type of distribution. A comparison of the normal and lognormal median reveals that the two are very similar in most cases (Fig. 10a). Therefore, for simplicity, the crack index was recalculated using the normal median in place of the lognormal median. The correlation of the new crack index was still quite strong, with only a decrease of 0.02 in the  $R^2$  value (Fig. 10b). This “normal crack index” is thus a simpler alternative which still may be used to explain strength loss in LME susceptible welds.

## 4 Conclusions

The current work proposes the crack index to quantify LME cracking severity based on crack length, crack frequency, and sheet thickness. The crack index was shown to have linear relationship with the loss in tensile lap shear strength. As such, it is the first cracking metric that has successfully linked crack severity to weld performance. The crack index was shown to quantify differences in cracking populations with more confidence than previously used cracking statistics (mean crack length, number of cracks, 95th percentile crack length) due to its lower associated error. The crack index is calculated using the lognormal median crack length as a metric of crack size, the number of cracks to account for the effect of crack location, and the sheet thickness as a normalization factor.

Fig. 10 a Comparison of normal and lognormal median. b Relationship between crack index calculated with normal median and strength loss



Normal median may be used in place of lognormal median to simplify the analysis.

**Acknowledgements** The authors would like to acknowledge the support of the Natural Science and Engineering Research Council of Canada and the International Zinc Association.

**Publisher's note** Springer Nature remains neutral with regard to jurisdictional claims in published maps and institutional affiliations.

## References

- Cooper AI (2015) Materials chemistry: cooperative carbon capture. *Nature* 519:294–295
- Jakob M, Hilaire J (2015) Unburnable fossil-fuel reserves. *Nature* 517:150–152. <https://doi.org/10.1038/517150a>
- McNutt M (2013) Climate change impacts. *Science* (80-) 341:435. <https://doi.org/10.1126/science.1243256>
- Creutzig F, Jochem P, Edelenbosch OY, Mattauich L, Vuuren DP, McCollum D, Minx J (2015) Transport: a roadblock to climate change mitigation? *Science* 350:911–912. <https://doi.org/10.1126/science.aac8033>
- Parkes D, Xu W, Westerbaan D, Nayak SS, Zhou Y, Goodwin F, Bhole S, Chen DL (2013) Microstructure and fatigue properties of fiber laser welded dissimilar joints between high strength low alloy and dual-phase steels. *Mater Des* 51:665–675. <https://doi.org/10.1016/j.matdes.2013.04.076>
- Parkes D, Westerbaan D, Nayak SS, Zhou Y, Goodwin F, Bhole S, Chen DL (2014) Tensile properties of fiber laser welded joints of high strength low alloy and dual-phase steels at warm and low temperatures. *Mater Des* 56:193–199. <https://doi.org/10.1016/j.matdes.2013.10.087>
- Zhang H, Senkara J (2006) Electrothermal processes of welding. In: Resistance welding: fundamentals and applications. CRC Press, Boca Raton, pp 19–57
- Ashiri R, Haque MA, Ji CW, shamanian M, Salimijazi HR, Park YD (2015) Supercritical area and critical nugget diameter for liquid metal embrittlement of Zn-coated twinning induced plasticity steels. *Scr Mater* 109:6–10. <https://doi.org/10.1016/j.scriptamat.2015.07.006>
- Kim YG, Kim IJ, Kim JS et al (2014) Evaluation of surface crack in resistance spot welds of Zn-coated steel. *Japan Inst Met Mater* 55: 171–175. <https://doi.org/10.2320/matertrans M2013244>
- Tolf E, Hedegård J, Melander A (2013) Surface breaking cracks in resistance spot welds of dual phase steels with electrogalvanised and hot dip zinc coating. *Sci Technol Weld Join* 18:25–31. <https://doi.org/10.1179/1362171812Y.0000000068>
- Choi D-Y, Sharma A, Uhm S-H, Jung JP (2018) Liquid metal embrittlement of resistance spot welded 1180 TRIP steel: effect of electrode force on cracking behavior. *Met Mater Int* 25:219–228. <https://doi.org/10.1007/s12540-018-0180-x>
- Barthelmie J, Schram A, Wesling V (2016) Liquid metal embrittlement in resistance spot welding and hot tensile tests of surface-refined TWIP steels. *IOP Conf Ser Mater Sci Eng* 118:012002. <https://doi.org/10.1088/1757-899X/118/1/012002>
- Beal C, Kleber X, Fabregue D, Bouzekri M (2012) Embrittlement of a zinc coated high manganese TWIP steel. *Mater Sci Eng A* 543: 76–83. <https://doi.org/10.1016/j.msea.2012.02.049>
- Saha DC, Chang I, Park Y-D (2014) Heat-affected zone liquation crack on resistance spot welded TWIP steels. *Mater Charact* 93:40–51. <https://doi.org/10.1016/j.matchar.2014.03.016>
- Gaul H, Weber G, Rethmeier M (2011) Influence of HAZ cracks on fatigue resistance of resistance spot welded joints made of advanced high strength steels. *Sci Technol Weld Join* 16:440–445. <https://doi.org/10.1179/1362171810Y.0000000031>
- Benlatreche Y, Ghassemi-Armaki H, Duchet M, et al (2017) Spot-weld integrity of Zn-coated 3rd gen. Advanced high strength steels in presence of LME. *Int Automot Body Congr*
- Jiang C, Thompson AK, Shi MF, et al (2003) Liquid metal embrittlement in resistance spot welds of AHSS steels. *AWS Prof Progr*
- Yan B, Zhu H, Lalam S et al (2004) Spot weld fatigue of dual phase steels. *SAE Tech Pap*. <https://doi.org/10.4271/2004-01-0511>
- Choi D-Y, Uhm S-H, Enloe CM et al (2017) Liquid metal embrittlement of resistance spot welded 1180TRIP steel - effects of crack geometry on weld mechanical performance. *Contrib Pap from Mater Sci Technol* 2017:454–462
- DiGiovanni C, Biro E, Zhou N (2018) Impact of liquid metal embrittlement cracks on resistance spot weld static strength. *Sci Technol Weld Join* 24:1–7. <https://doi.org/10.1080/13621718.2018.1518363>
- DiGiovanni C, Biro E, Zhou NY (2018) Effect of liquid metal embrittlement cracks on resistance spot weld fracture path. *Sheet Met Weld Conf XVIII* 24:218–224. <https://doi.org/10.1080/13621718.2018.1518363>
- Ashiri R, Shamanian M, Salimijazi HR, Haque MA, Bae JH, Ji CW, Chin KG, Park YD (2016) Liquid metal embrittlement-free welds of Zn-coated twinning induced plasticity steels. *Scr Mater* 114:41–47. <https://doi.org/10.1016/j.scriptamat.2015.11.027>
- Wintjes E, Macwan A, Biro E, Zhou YN (2018) Effect of multi-pulse welding on LME severity in RSW joints. *Sheet Met Weld Conf XVIII*
- Frei J, Rethmeier M (2018) Susceptibility of electrolytically galvanized dual-phase steel sheets to liquid metal embrittlement during resistance spot welding. *Weld World* 62:1031–1037. <https://doi.org/10.1007/s40194-018-0619-1>
- American Welding Society (2012) American Welding Society: test method for evaluating the resistance spot welding behavior of automotive sheet steel materials (AWS D 89M). 1–107
- Beal C (2012) Mechanical behaviour of a new automotive high manganese TWIP steel in the presence of liquid zinc [dissertation]. Insa Lyon
- Taylor JR (1997) An introduction to error analysis: the study of uncertainties in physical measurements, 2nd ed. University Science Books, Sausalito, CA
- Efron B (1979) Bootstrap methods: another look at the jackknife. *Ann Stat* 7:1–26. <https://doi.org/10.1214/aos/1176344552>